

## **Operational Strategies of Pulsed Electrolysis to Enhance Multi-Carbon Product Formation in Electrocatalytic CO<sub>2</sub> Reduction**

Takashi Ito,<sup>1</sup> Jithu Raj,<sup>1</sup> Tianyu Zhang,<sup>1</sup> Soumyabrata Roy,<sup>2</sup> Jingjie Wu<sup>1\*</sup>

<sup>1</sup>Department of Chemical and Environmental Engineering, University of Cincinnati, Cincinnati, OH, 45221, USA

<sup>2</sup>Department of Materials Science and NanoEngineering, Rice University, Houston, TX 77005, USA

\*Corresponding author: [jingjie.wu@uc.edu](mailto:jingjie.wu@uc.edu)

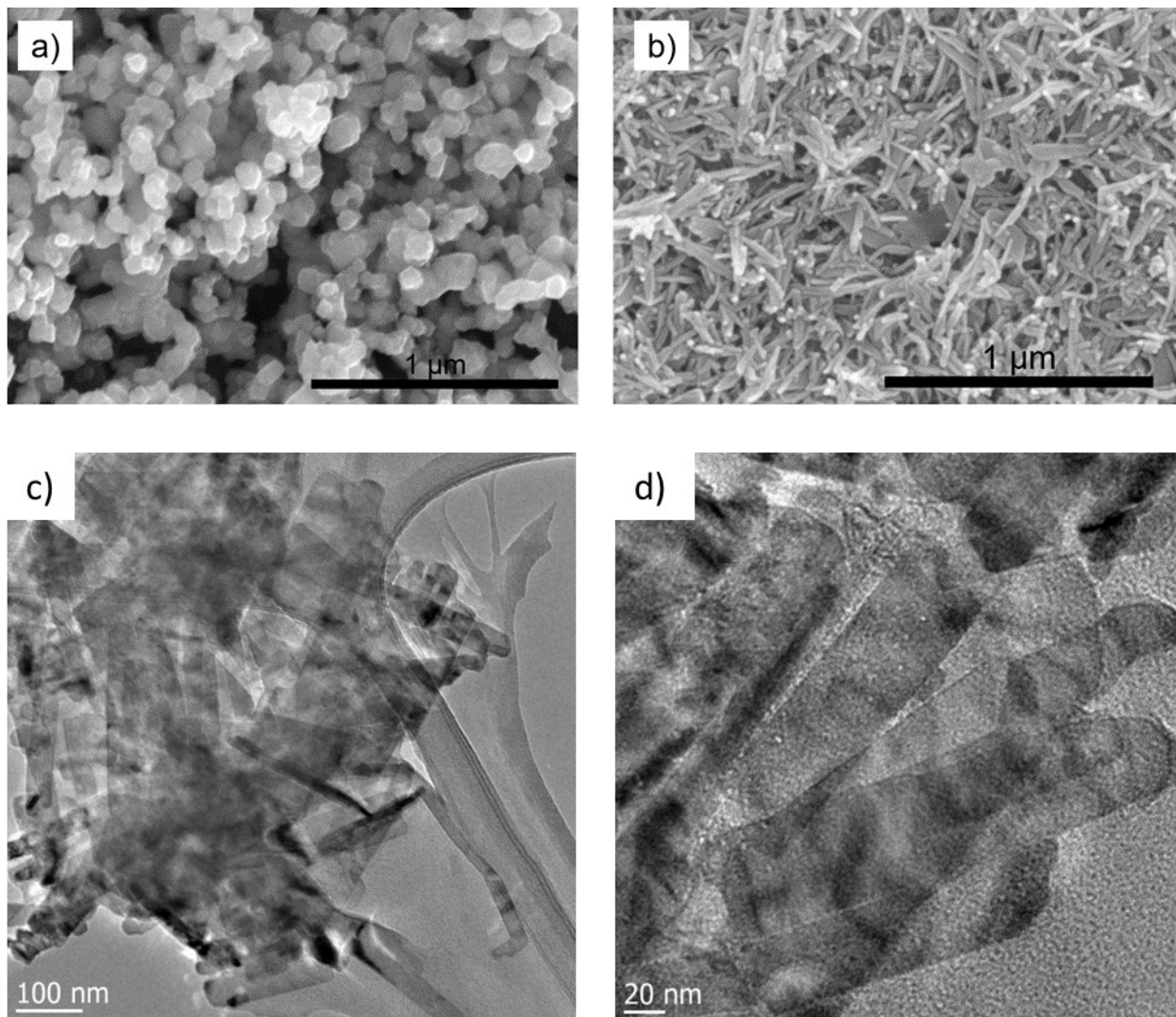


**Figure S1.** SEM images of (a) Cu nanoparticles (Cu NPs) and (b) CuO nanowires (CuO NWs). (c-d) TEM image of CuO NWs.

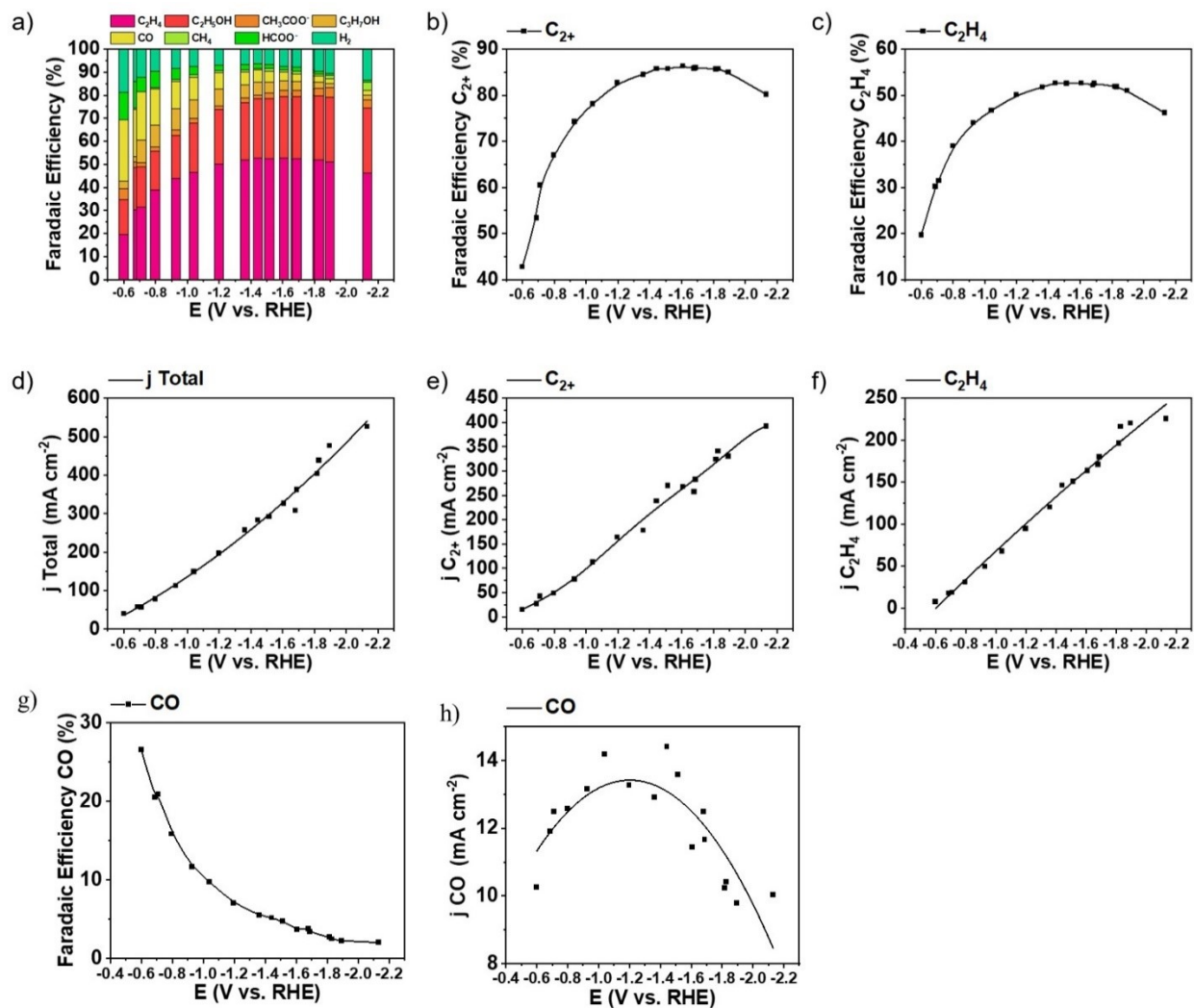


**Figure S2.** Static electrolysis results of Cu NP GDEs in the flow cell. (a) Faradic efficiency of all eCO<sub>2</sub>RR products, (b) Faradaic efficiency of C<sub>2+</sub> products, (c) Faradaic efficiency of C<sub>2</sub>H<sub>4</sub>, (d) Total current density of all eCO<sub>2</sub>RR products, (e) Partial current density for C<sub>2+</sub> products, (f) Partial current density for C<sub>2</sub>H<sub>4</sub>, (g) Faradaic efficiency of CO, (h) Partial current density for CO.

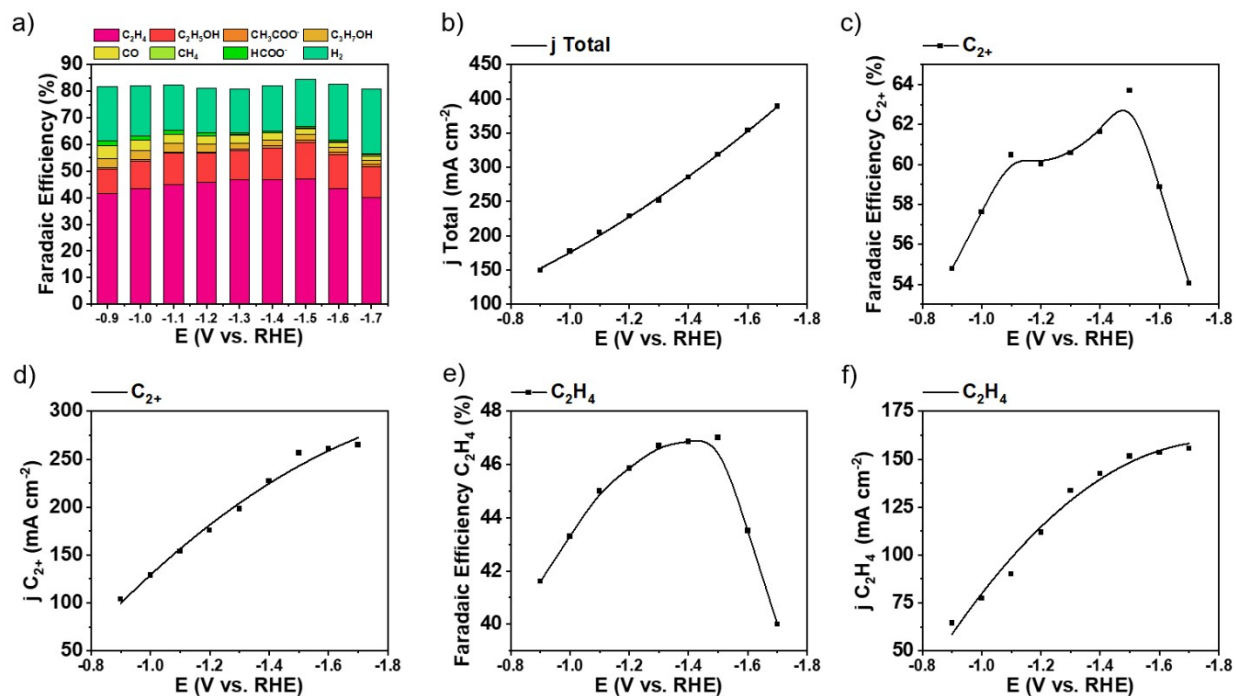


**Figure S3.** Static electrolysis results of CuO NW GDEs in the flow cell. (a) Faradic efficiency of all CO<sub>2</sub>RR products, (b) Total current density of all CO<sub>2</sub>RR products, (c) Faradaic efficiency of C<sub>2+</sub> products, (d) Partial current density for C<sub>2+</sub> products, (e) Faradaic efficiency of C<sub>2</sub>H<sub>4</sub>, (f) Partial current density for C<sub>2</sub>H<sub>4</sub>.

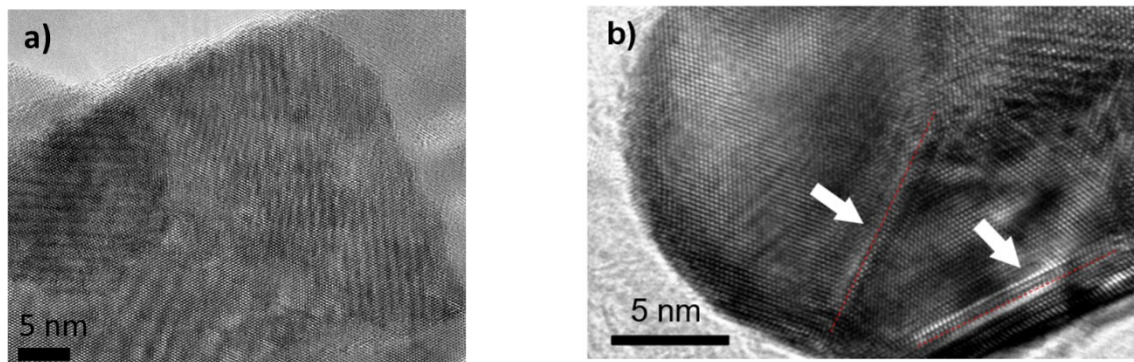


**Figure S4.** TEM images of CuO NWs (a) before and (b) after the pulse eCO<sub>2</sub>RR

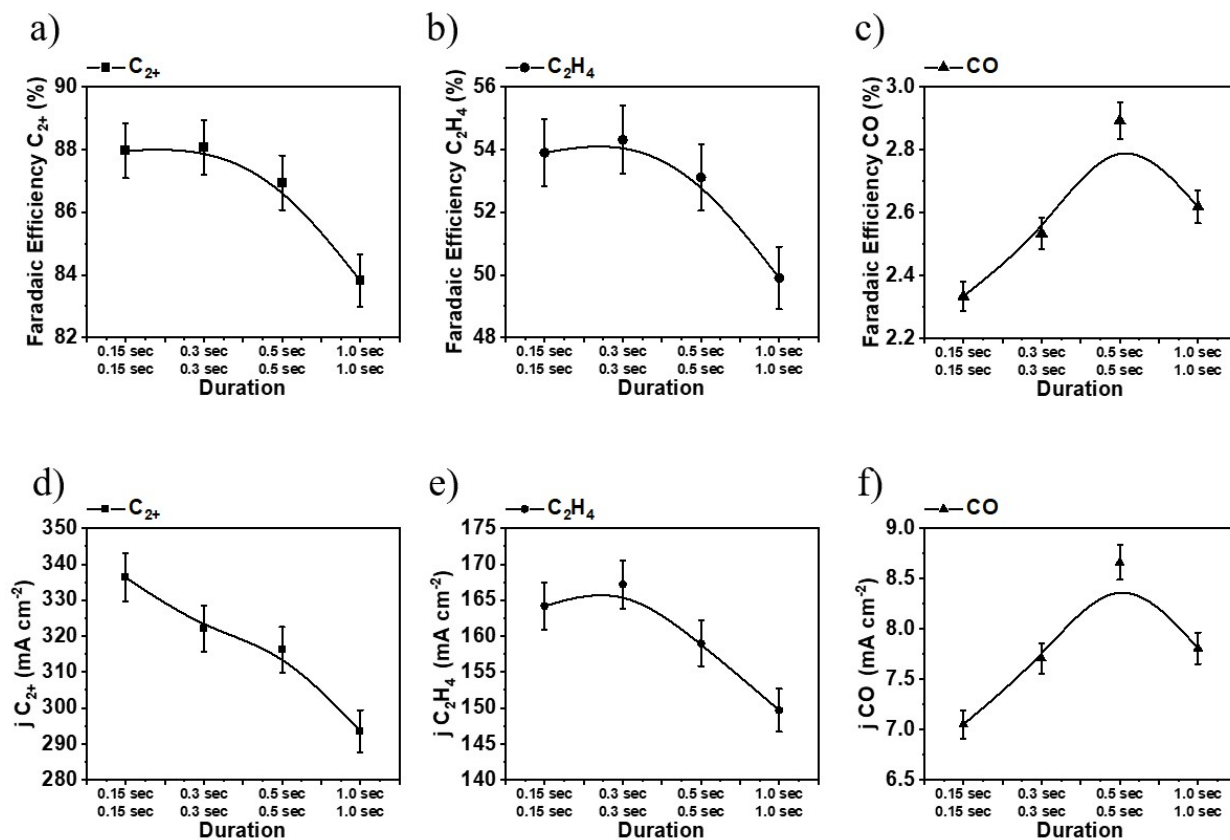


**Figure S5.** Optimization of pulse duration for the flow cell with  $E_{c1} = -1.2$  V and  $E_{c2} = -1.5$  V. The selected anodic/cathodic durations are 0.15 sec/0.15 sec, 0.3 sec/0.3 sec, 0.5 sec/0.5 sec, and 1.0 sec/1.0 sec. (a) Faradaic efficiency of C<sub>2+</sub> products, (b) Faradaic efficiency of C<sub>2</sub>H<sub>4</sub> (c) Faradaic efficiency of CO, (d) Current density for C<sub>2+</sub> products, (e) Current density for C<sub>2</sub>H<sub>4</sub>, and (f) Current density for CO. Cu NPs were used as the catalyst. The error bar represents the standard deviation of performance for at least three independent electrodes.

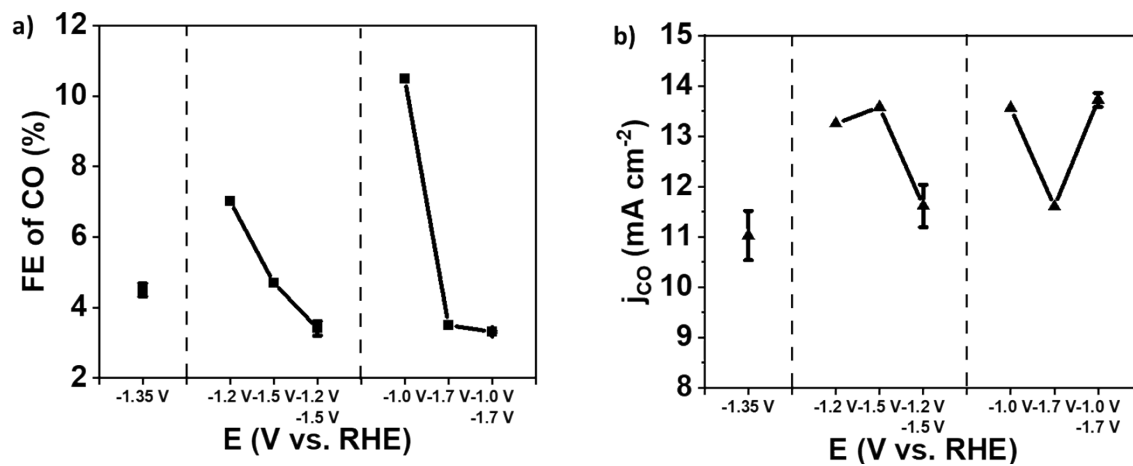


**Figure S6.** Comparison of pulse electrolysis for Cu NP GDEs in the flow cell with the potential setup of -1.2 V/-1.5 V and -1.0 V/-1.7 V with static electrolysis at potentials of -1.0 V, -1.2 V, -1.35 V, -1.5 V, and -1.7 V. The error bar represents the standard deviation of performance for at least three independent electrodes.

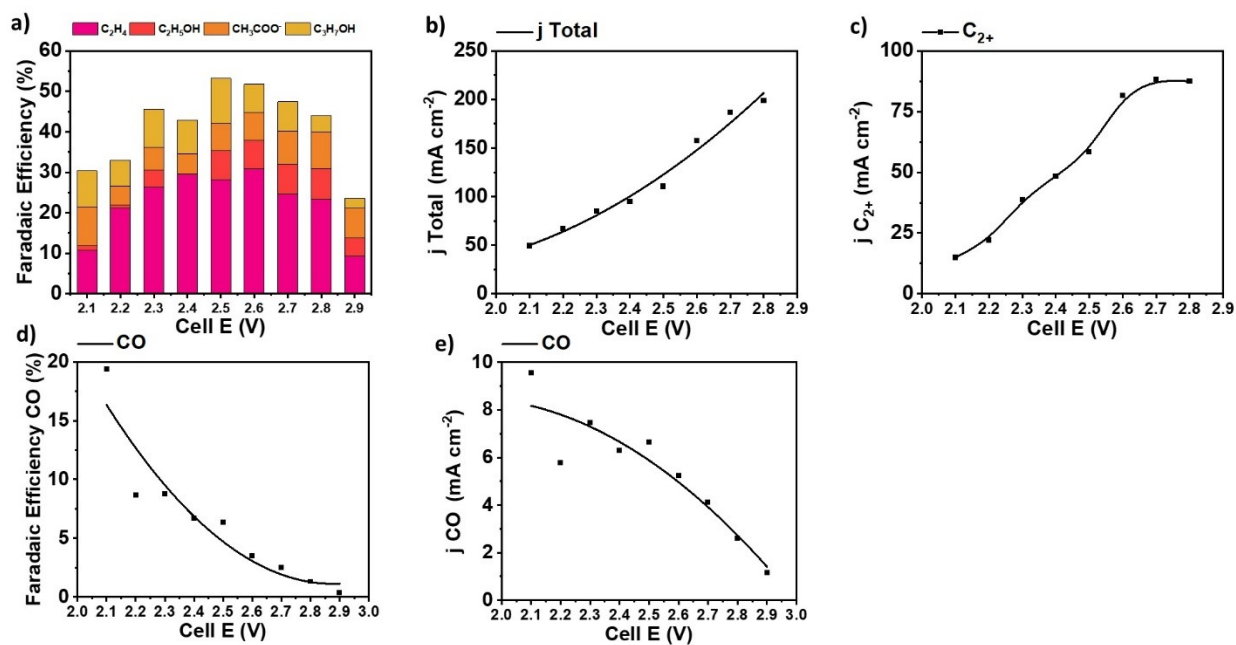


**Figure S7.** Potentiostatic electrolysis results of Cu NP GDEs in the MEA cell. (a)  $C_{2+}$  product distribution, (b) Total current density for all products, (c) Partial current density for  $C_{2+}$  products, (d) Faradaic efficiency for CO, and (e) Partial current density for CO.



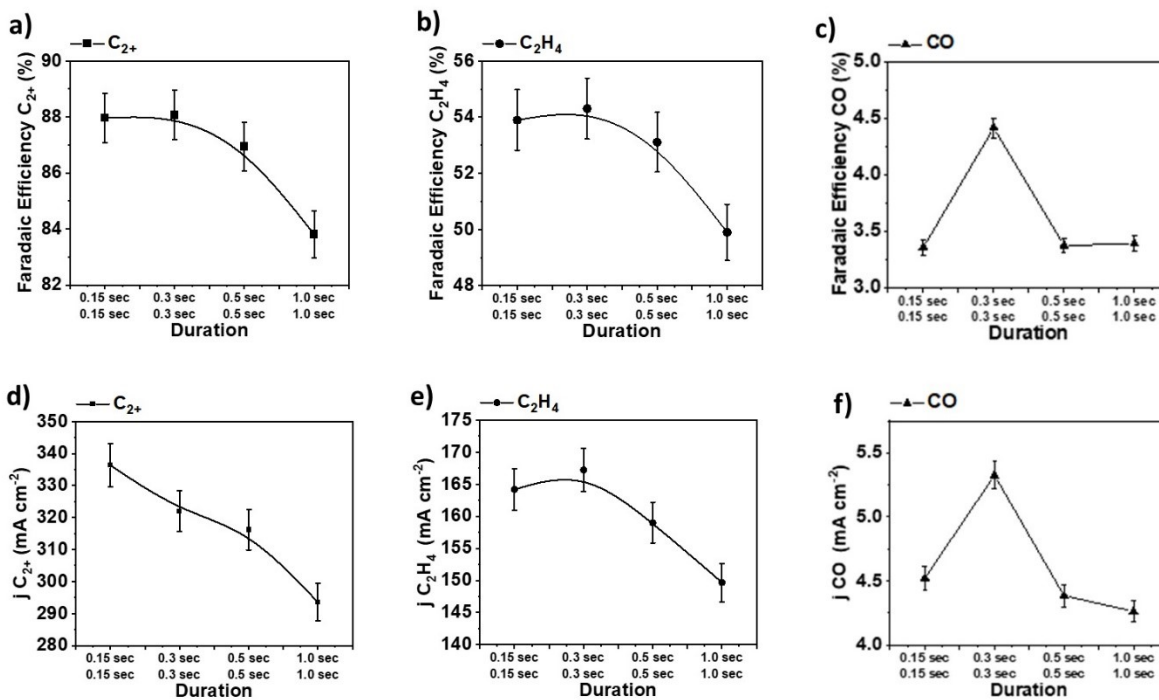


**Figure S8.** Optimization of pulse duration for the MEA cell using cell voltage  $E_{c1} = 2.1$  V and  $E_{c2} = 2.5$  V over Cu NP GDEs. The selected anodic/cathodic durations are 0.15 sec/0.15 sec, 0.3 sec/0.3 sec, 0.5 sec/0.5 sec, and 1.0 sec/1.0 sec. (a) Faradaic efficiency of  $C_{2+}$  products, (b) Faradaic efficiency of  $C_2H_4$ , (c) Faradaic efficiency of CO, (d) Current density for  $C_{2+}$  products, (e) Current density for  $C_2H_4$ , and (f) Current density for CO. The error bar represents the standard deviation of performance for at least three independent electrodes.

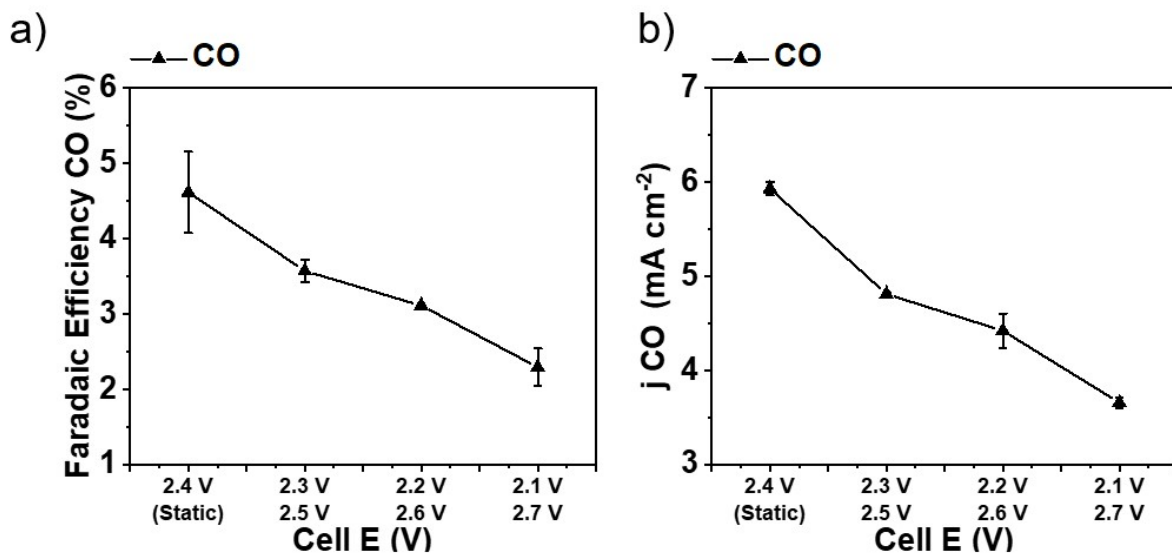


**Figure S9.** Comparison of pulse electrolysis for Cu NP GDEs in the MEA cell with alternating cell voltage of 2.3 V/2.5 V, 2.2 V/2.6 V, and 2.1 V/2.7 V with static electrolysis at an average cell voltage of 2.4 V. (a) Faradaic efficiency of CO and (b) Partial current density for CO. The error bar represents the standard deviation of performance for at least three independent electrodes.

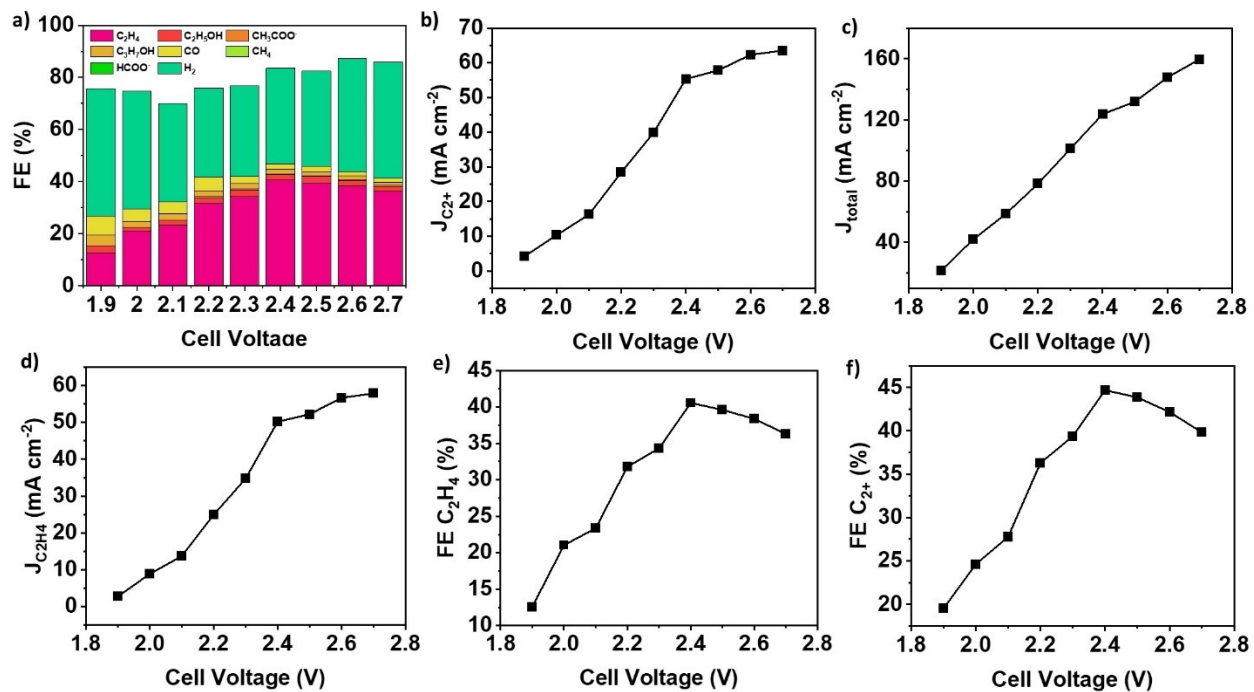


**Figure S10.** Performance of potentiostatic electrolysis for CuO NW GDEs in the MEA cell. (a) Product distribution, (b) Partial current density for  $C_{2+}$  products, (c) Total current density for all products, (d) Partial current density of  $C_2H_4$ , (e) FE of  $C_{2+}$  products, (f) FE of  $C_2H_4$ .

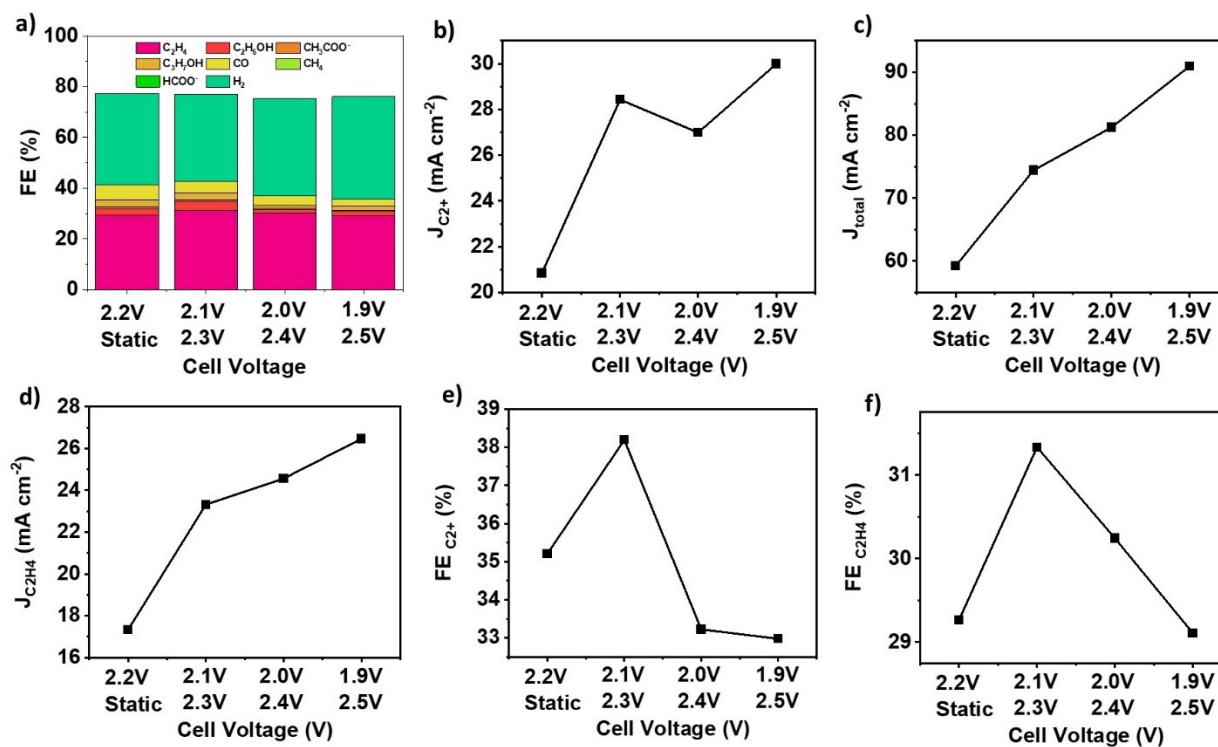


**Figure S11.** Performance of pulsed electrolysis for CuO NW GDEs in the MEA cell with alternating cell voltage of 2.1 V/2.3 V, 2.0 V/2.4 V and 1.9 V/2.5 V and  $t_{c1} = t_{c2} = 0.3$  seconds, and comparison to static electrolysis at an time-average cell potential of 2.2 V. (a) Product distribution, (b) Partial current density for  $C_{2+}$  products, (c) Total current density for all products, (d) Partial current density of  $C_2H_4$ , (e) FE of  $C_{2+}$  products, (f) FE of  $C_2H_4$ .

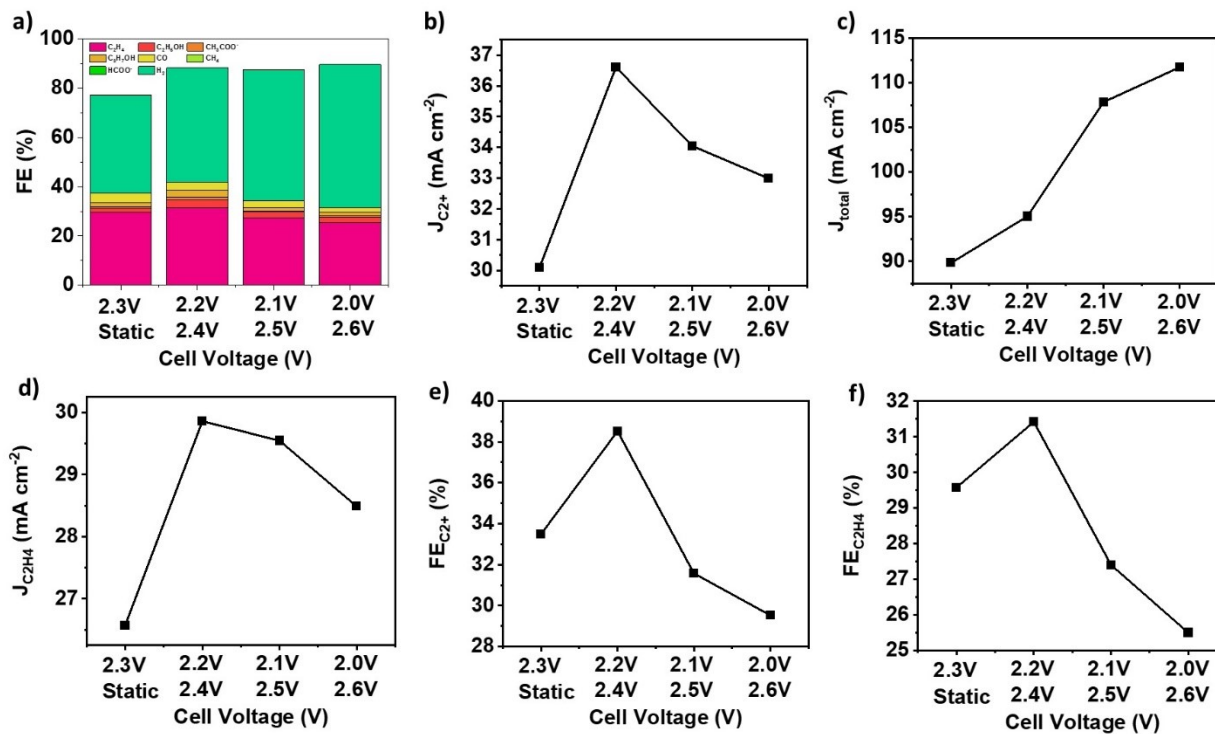


**Figure S12.** Performance of pulsed electrolysis for CuO NW GDEs in the MEA cell with alternating cell voltage of 2.2 V/2.4 V, 2.1 V/2.5 V and 2.0 V/2.6 V and  $t_{c1} = t_{c2} = 0.3$  seconds, and comparison to static electrolysis at an time-average cell potential of 2.2 V. (a) Product distribution, (b) Partial current density for  $C_{2+}$  products, (c) Total current density for all products, (d) Partial current density of  $C_2H_4$ , (e) FE of  $C_{2+}$  products, (f) FE of  $C_2H_4$ .

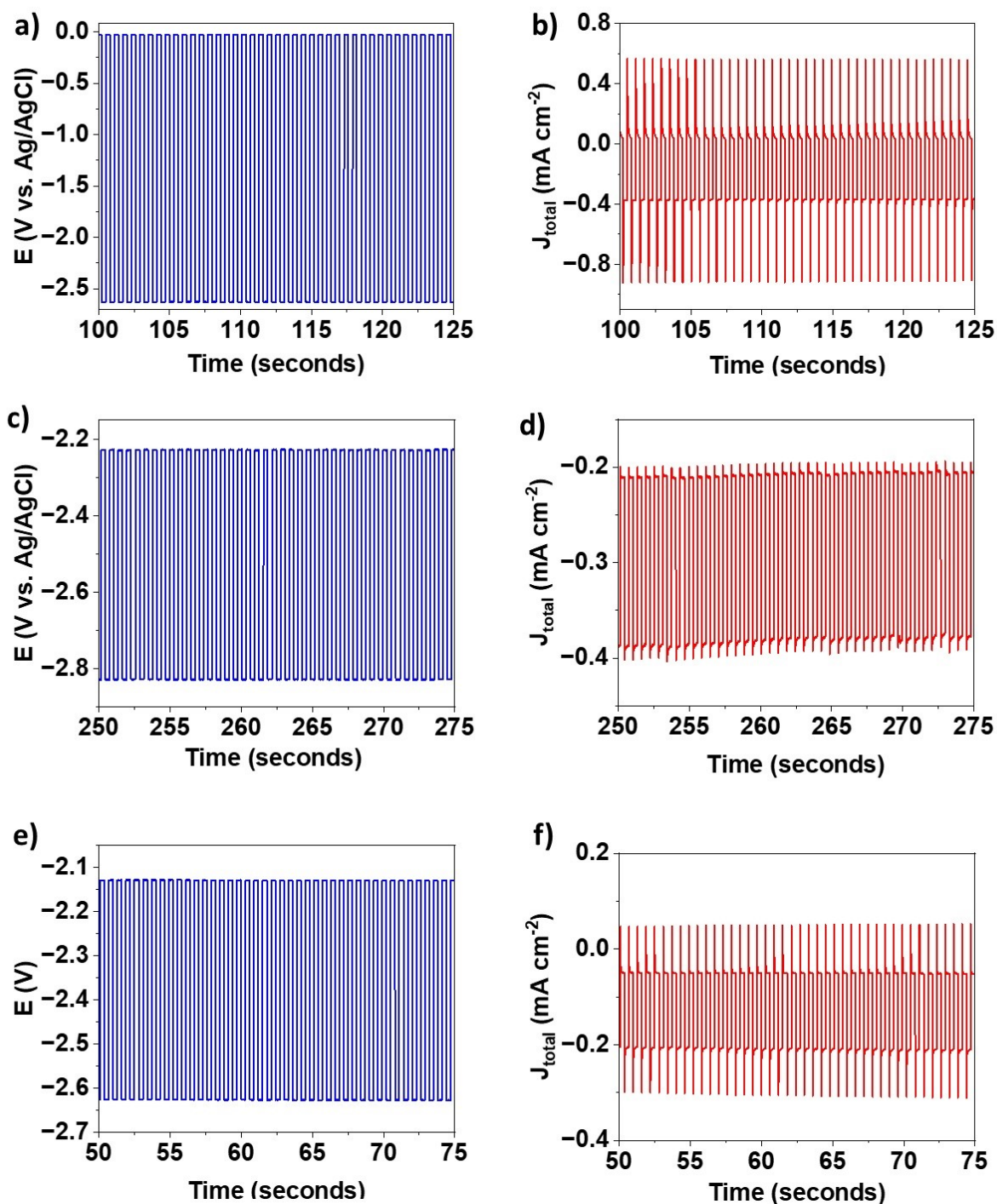


**Figure S13.** Representative potential versus time and current versus time plots, respectively for (a) and (b) Cu NP in flow cell under  $E_a/E_c$  mode, (c) and (d) Cu NP in flow cell under  $E_{c1}/E_{c2}$  mode, (e) and (f) Cu NP in MEA cell under  $E_{c1}/E_{c2}$  mode.

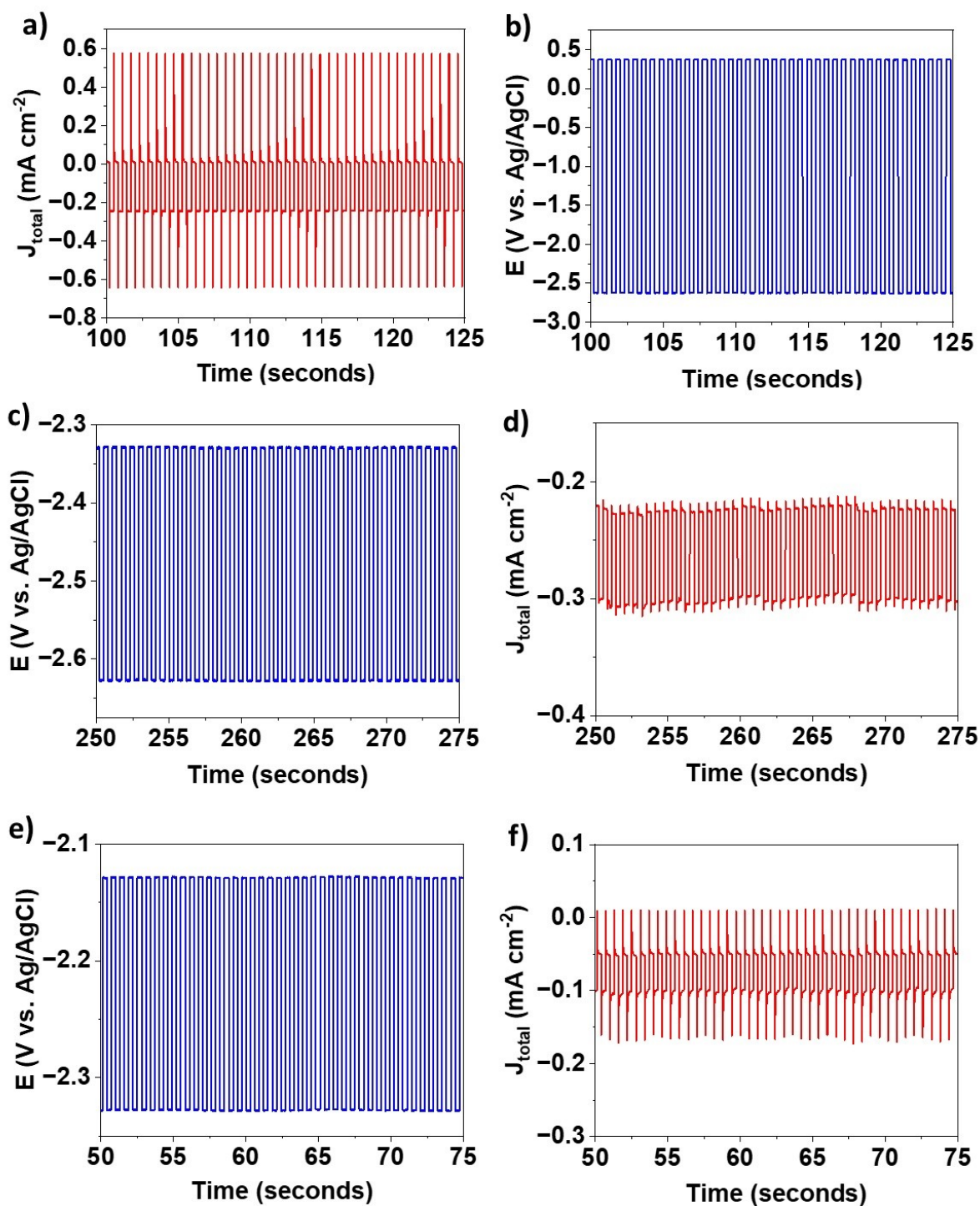


**Figure S14.** Representative potential versus time and current versus time plots, respectively for (a) and (b) CuO NW in flow cell under  $E_a/E_c$  mode, (c) and (d) CuO NW in flow cell under  $E_{c1}/E_{c2}$  mode, (e) and (f) CuO NW in MEA cell under  $E_{c1}/E_{c2}$  mode.

## Supplemental Note 1

### Calculations for pulse duration

Pulse duration is also one of the key aspects to be considered for pulse electrolysis. The flexibility of pulse electrolysis is that the user can select durations for each potential independently. Pulse frequency is calculated based on the duration of each potential. The pulse electrolysis causes the non-faradaic process and double-layer charging by switching potentials. The optimal duration needs to be sufficiently long to avoid the effect of double-layer charging. The RC time constant for double-layer charging can be calculated with the cell resistance and the capacitance of the electrode. These data are generally available based on the eCO<sub>2</sub>RR experiment and the cyclic voltammetry with a potentiostatic/galvanostatic station. The reported RC time constant for the double layer charging is approximately 6-30 milliseconds<sup>1-3</sup> While the oxidation of catalysts is the crucial factor in using pulse electrolysis with  $E_a/E_c$ , the required period for oxidation of catalysts needs to be considered as well. Previous studies reveal that the oxidized catalysts were observed at 1 second or longer pulses, however, the shorter duration (< 1 sec) of anodic potential does not show clear trends due to the difference in experimental setup including electrode area. Moreover, the duration of the pulsed electrolysis with different cathodic potentials also influences the performance. The theoretical modeling discovered that the longer less cathodic potential causes the suppression of C<sub>2+</sub> product formation and favors favor C<sub>1</sub> product formation and H<sub>2</sub> formation due to the weakly acidic local environment. Although the theoretical and experimental studies show the optimal durations of pulse electrolysis, the durations of anodic and cathodic potentials to oxidize catalysts, reconstruct catalyst morphology, and change the local environment strongly depend on the reaction area, electrolysis cell types, electrochemical systems, and many more.



### **Time for double layer charging in our flow cell:**

$$\tau = \text{Resistance} \times \text{Capacitance} = 2.5 \, \Omega \times 3.6 \, \text{mF} = 9 \, \text{milli seconds}.$$

Where the resistance and capacitance were determined by fitting electrochemical impedance spectra data.

### **Residence time of CO<sub>2</sub>/CO in the flow cell:**

$$\text{Residence time} = \frac{\text{Channel Volume}}{\text{CO}_2 \text{ Flow Rate}} = \frac{1 \, \text{ml}}{20 \, \text{ml/min}} = 3 \, \text{seconds}.$$

### **References**

- 1 Kim, C., Weng, L.-C. & Bell, A. T. Impact of pulsed electrochemical reduction of CO<sub>2</sub> on the formation of C<sub>2</sub>+ products over Cu. *ACS Catalysis* **10**, 12403-12413 (2020).
- 2 Ha, S. & Doblhofer, K. The electrochemical interface between copper (111) and aqueous electrolytes. *Journal of Electroanalytical Chemistry* **380**, 185-191 (1995).
- 3 DiDomenico, R. C. & Hanrath, T. Pulse Symmetry Impacts the C<sub>2</sub> Product Selectivity in Pulsed Electrochemical CO<sub>2</sub> Reduction. *ACS Energy Letters* **7**, 292-299, doi:10.1021/acseenergylett.1c02166 (2022).